

INVESTIGATION OF METALLIC NANOPARTICLES PRODUCED BY LASER ABLATION METHOD AND THEIR CATALYTIC ACTIVITY ON CVD DIAMOND GROWTH

ZAHRA KHALAJ^a, MAHMOOD GHORANNEVISS^{a,*}

ABSTRACT. The synthesis of high quality diamond films is one of the particular interests due to the material's outstanding physical and mechanical properties. In CVD diamond we found a new process parameter window where the growth of diamond films can be stabilized without the use of diamond powder on substrates. Using suitable catalyst and etching gas would enhance the diamond nucleation and therefore, increase the quality of the films. A laser ablation was conducted by using an optical system for producing the metallic nanoparticles. A light source with a first harmonic generator (FHG) of an Nd:YAG laser were used with the wavelength of 1064 nm, pulse duration: 6 ns and repetition rate of 10 Hz. Au and Ag nanoparticles were dried on the Si and glass wafers as a catalyst and etching treated by hydrogen plasma for 30 minutes. Topography of the wafers was analyzed using Atomic Force Microscopy (AFM) and shows a good distribution of the nanoparticles on the substrate surface. Diamond films were deposited on substrates coated metal using a Hot Filament Chemical Vapor Deposition (HFCVD) system. Crystallinity of the samples was observed by X-ray diffraction (XRD) method. Results show good quality diamond crystals with crystallinity of (311) structures, grown on substrate surface. According to the Scherrer formula, the grain size (L_{hkl}) of diamond nano crystals were calculated by $L_{hkl} = K\lambda/B \cos\theta_{hkl}$, where B is the FWHM in radians and λ is the wavelength in nm.

Keywords: Nd:YAG laser, NNP, CVD diamond.

INTRODUCTION

Carbon is one of the most important natural elements, which has several allotropes [1,2] such as carbon nanotubes [3], carbon nanowalls [3], diamond-like carbon [4], etc. Among different hybridizations [5], the sp^3 form is involved in the diamond structure. Due to its outstanding properties, diamond is the unique material with various applications in life and technology. By developing the Chemical Vapor Deposition (CVD) technology, the deposition of nanocrystalline diamond films (NDFs) by various CVD techniques has become the topic of wide research [6-9]. The quality and purity of nano structures in CVD techniques are very important. There are some possibilities

^a Plasma Physics Research Center, Science and Research Branch, Islamic Azad University, Tehran, Iran, *Correspondent: Ghoranneviss@gmail.com

for increasing the quality and quantity of these deposits. The nucleation and growth of diamond coating can be dramatically improved with different surface treatments [10]. There are several methods for the enhancement of diamond nucleation, including mechanical and chemical treatment processes. One of the effective methods is the use of a catalyst layer for diamond deposition [10]. Using a catalyst layer can increase the rate of diamond nucleation and provide a carbon diffusion barrier layer to increase the needed carbon concentration for diamond nucleation [11, 12]. Using suitable catalyst and etching gas can enhance the diamond nucleation and therefore, increase the quality of the films.

In this paper, gold and silver nanoparticles were produced using laser ablation method and dried on the Si and glass wafers as a catalyst and compared with silicon with no pretreatments. All samples were etching treated by hydrogen plasma by Plasma Enhanced Chemical Vapor Deposition (PECVD) and grown using Hot Filament Chemical Vapor Deposition (HFCVD) system. The formation of metallic nanoparticles has been characterized by a variety of physical techniques such as, UV-vis spectroscopy and Atomic Force Microscopy (AFM). The crystallinity of the samples was studied by XRD ($\text{CuK}\alpha$, $\lambda=0.154\text{nm}$, D/Max=2200, X-ray diffractometer) analysis. Fourier transform infrared (FT-IR) spectroscopy was used to characterize the coating.

RESULTS AND DISCUSSION

MORPHOLOGY OF THE FILMS

Figure 1 shows the measured absorption bands of the pure Au and Ag nanoparticles. The solution of pure Au nanoparticles, prepared by the laser ablation method, shows a reddish brown in color. The color of the solution is yellow for the silver nanoparticles, obtained in acetone. A sharp Plasmon band attributable to silver nanoparticles was observed around 400 nm. Observe that the surface Plasmon bands display a symmetrical configuration.

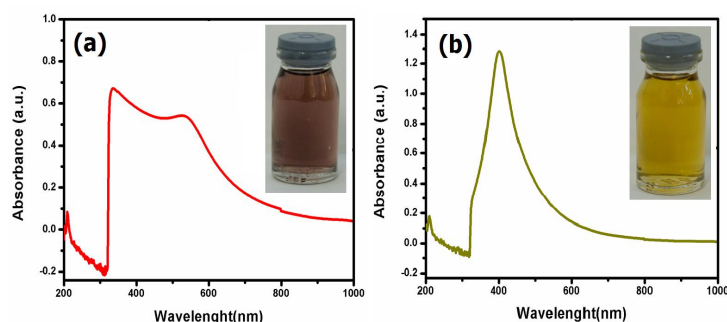


Figure 1. UV-vis spectra of (a) gold (b) silver, nanoparticles prepared by laser ablation in acetone solutions

Atomic force microscopy was performed on silicon coated nanoparticles in contact mode on $3\mu\text{m} \times 3\mu\text{m}$ area. Figure 2 shows 3D images of the silicon coated by gold (S_1) and silicon coated by silver (S_2). Three dimensional images in both samples show different topography, which result in different average roughness for each sample. Therefore, as we can see in Figure 2(b) the distribution of size for silver nanoparticles is homogeneous while the homogeneity is less for Au NPs, Figure 2(a).

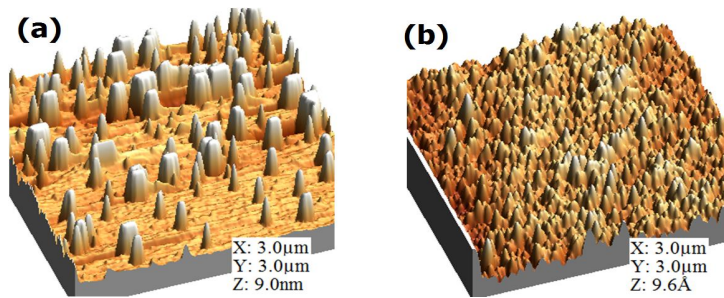


Figure 2. Three dimensional AFM images of silicon coated by (a) Gold and (b) silver nanoparticles.

Figure 3 shows the histograms of the size distribution of the metallic nanoparticles on the silicon surface. As the Gaussian diagram shows for S_2 , the distribution of the Ag nanoparticles on substrates is homogenous. This homogeneity is less for S_1 because of the sharp difference between the distribution sizes of the nanoparticles. Moreover, S_1 particles are rather isolated from each other while there is a continuous distribution for S_2 . This observation suggests that the particles seen at S_1 are fairly clusters of crystallites. In addition, the width of the peak in S_2 is larger than in S_1 . It means that there is a high distribution in size of nanoparticles in S_2 . Moreover surface roughness is low in this case.

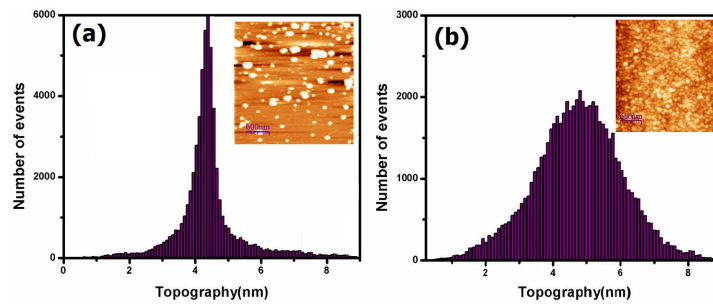


Figure 3. 2D AFM image and histogram of the size distribution of silicon coated by (a) gold and (b) silver nanoparticles.

The Root-Mean-Squared roughness (R_{rms}) of surface is one of the most important parameters for characterization of surface structure [4]:

$$R_{rms} = \sqrt{\frac{\sum_{n=1}^N (z_n - \bar{z})^2}{N-1}}$$

$$\bar{z} = \frac{1}{N} \sum_{n=1}^N z_n$$

with N being the number of data points [4]. The results of AFM studies after etching treatments are listed in Table 1.

Table 1. AFM studies of the silicon coated metallic particles

No.	Sample	Rms rough. (nm)	Ave. rough. (nm)	Ave. height
S_1	Si-Au	1.33	0.77	4.34
S_2	Si-Ag	0.19	0.15	0.63

The AFM results show that the RMS roughness of the samples decreases from S_1 to S_2 . Therefore the substrate surface becomes smoother which is suitable for diamond nucleation.

XRD patterns of the diamond crystals deposited for 120 minutes at 25 Torr are shown in Figure 4. Based on Figure 4, a diffraction peak was found in the spectra for S_1 at 92.10° . One can observe the spectrum is dominated by intense peaks located at $2\theta = 92.12^\circ$ for S_2 which could be identified with reflections from (311) plane of diamond. The Full Width Half Maximum (FWHM) of the diamond peaks could be used for distinguishing the quality of diamonds. The sharp peaks with small FWHM indicate high crystal quality. The FWHM (B) of these peaks was used to calculate the grain size (L_{hkl}) from the well-known Scherrer's equation:

$$L_{hkl} = \frac{K\lambda}{B \cos \theta_{hkl}}$$

Here $K=0.9$, $\lambda=0.154\text{nm}$ and θ is the Bragg angle.

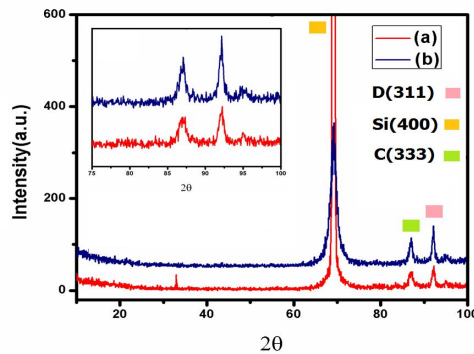


Figure 4. The XRD pattern for NCD films on: (a) S_1 and (b) S_2

Table 2 shows some calculations for the grain size of the diamond in both samples.

Table 2. XRD studies for the diamond crystals grown on different substrates

Sample	Operating Pressure (Torr)	Orientation of plane	2Θ (deg.)	FWHM (deg.)	$\Delta(2\Theta)\cos(\Theta) \times 10^{-3}$ (rad.)	T (nm)
S ₁	25	(311)	92.10	0.7210	0.0086	16.11
S ₂	25	(311)	92.12	0.3302	0.0039	35.53

Due to the lower FWHM and higher intensity, the quality of the diamond in S₂ is better than S₁. In addition, the AFM data show that the RMS in S₁ and S₂ was 1.33nm and 0.19 nm, respectively. Therefore, the substrate surface in S₂ was smoother than S₁ which is more suitable for diamond growth. That is AFM and XRD results confirm each other. There was no peak observed for diamond coating on pure silicon.

Fourier Transform Infrared (FTIR) spectroscopy is a spectroscopic technique used to characterize the chemical bonds, molecular structures and C-H_n (n=1, 2, 3) bonding configurations in carbon materials. The typical infrared spectra of the diamond films deposited on S₂ substrate, in the range of 1000-4000 cm⁻¹, are shown in Figure 5. It shows an absorption band in CVD diamond in the "C-H stretch" region, with the peak at 2932.49 cm⁻¹, which is believed to be caused by symmetric C-H₂ stretching vibrations.

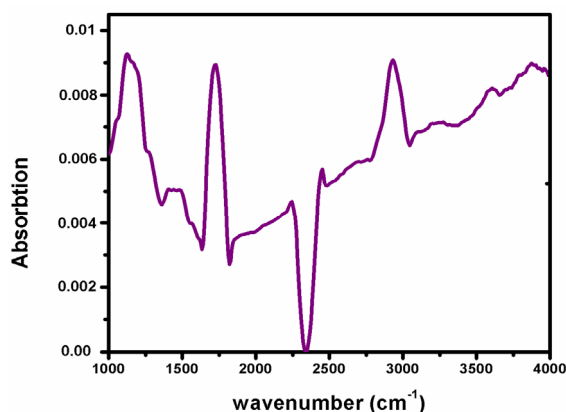


Figure 5. Typical FTIR absorbance spectra of the diamond films grown on S₂

EXPERIMENTAL DETAILS AND METHODOLOGY

SUBSTRATE TREATMENTS AND FILM SYNTHESIS

Diamond films were synthesized on P-type Silicon wafers (100) in the size of 5mm×5mm. All the substrates were cleaned in acetone and rinsed with ethanol prior to deposition. Two methods were used for diamond films, ND: YAG laser and CVD systems. Au and Ag nanoparticles were prepared by laser ablation of high purity targets in acetone using a first harmonic (1064 nm) Nd:YAG pulse laser with a repetition rate of 10 Hz, pulse width of 6 ns and a fluency of 1.5 J/cm². The laser beam strikes the surface vertically after passing throughout an optical window and the liquid. Figure 6 shows a schematic diagram for the laser ablation of a target in liquid. Au and Ag nanoparticles were dried on the Si wafers and were named S₁ and S₂ respectively.

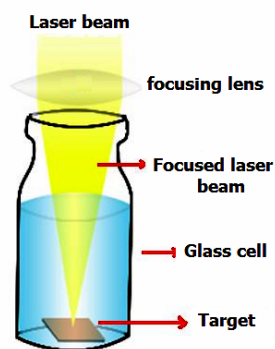


Figure 6. Schematic diagram for the laser ablation of target in liquid phase

CVD diamond growth was performed on the DC-Plasma Enhanced Chemical Vapor Deposition (PECVD) and Hot Filament Chemical Vapor Deposition (HFCVD) systems. S₁, S₂ and a silicon substrate with no catalyst pretreatments (S₃) were load to the central part of the DC-PECVD which is a cylindrical chamber with a diameter of 28cm consisting of a base and a cover. On the top of the system cover the DC source is flanged. The chamber can be opened for substrate handling by vertical shifting the aluminum cover on top. The temperature of the substrates is monitored by a thermocouple. A Hydrogen gas was inserted to the system for 30 minutes to create suitable sites for diamond growth. Using H₂ as etching gas would increase the diamond nucleation by creating suitable sites on substrate surface.

The substrate temperature, flow rate, and etching pressure were about: 200°C, 135 sccm, and 10 Torr, respectively. The samples were moved to the HFCVD system for diamond growth. This system consists of a horizontal stainless steel (S.S.316) cylinder as a reaction chamber, a furnace and filament (see Figure 7) [13].

After getting the base pressure, we feed the substrate with source gases through a steel nozzle. The substrate temperature, T_s , was increased up to 600°C, gradually. The temperature of the filament, T_F , was increased up to 1600°C. A combination of CH_4/H_2 with 5% flow ratio was fed into the reaction chamber. The reaction pressure and maximum temperature of the filament for the growth were 25 Torr and $\approx 1700^\circ\text{C}$, respectively. The duration of time was 120 minutes. Due to the high ionization energy of the hot filament, good quality diamond films were produced.

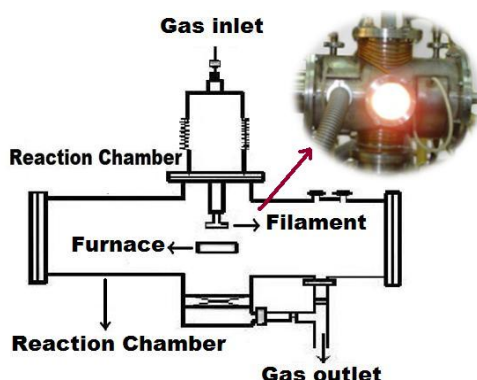


Figure 7. Schematic diagram of the HFCVD system

CONCLUSION

In this work, we have investigated the growth of diamond nanocrystals on silicon substrate with a new method. Using ND: YAG laser, we produced Au and Ag nanoparticles in acetone solution. Silicon wafers coated by Au and Ag nanoparticles were compared by pure silicon with no treatments. Using DC-PECVD and HFCVD techniques, high quality diamond nanocrystals with crystallinity of (311) were grown on pretreated substrates. The XRD patterns show the diamond nanocrystals grown on Si covered Ag have a higher quality, as shown by their high intensity and small FWHM in diamond peaks. The FTIR analysis for silicon coated by Ag shows an absorption band in CVD diamond with the peak at 2932.49 cm^{-1} , which is believed to be caused by symmetric C-H_2 stretching vibrations. There was no diamond coating on pure silicon.

The results show that the ionization rate of reaction gases and substrate pretreatments have a great influence on diamond nucleation. Using gold and silver coatings on silicon substrates had a good influence on diamond nucleation in this experiment.

ACKNOWLEDGEMENTS

The authors would like to thank the Iran National Science Foundation (INSF) for supporting this project.

REFERENCES

1. N.G. Shang, F.C.K. Au, X.M. Meng, C.S. Lee, I. Bello, S.T. Lee, *Chem. Phys. Lett.*, **2002**, 358, 187-191.
2. E.C. Almeida, A.F. Azevedo, M.R. Baldan, N.A. Braga, J.M. Rosolen, N.G. Ferreira, *Chem. Phys. Lett.*, **2007**, 438, 47-52.
3. P. Alizadeh Eslami, M. Ghoranneviss, Sh. Moradi, P. Abroomand Azar, S. Abedini Khorrami, S. Nasiri Laheghi, *Fuller Nanotub Car N*, **2011**, 19, 237-249.
4. E. Vaghri, Z. Khalaj, M. Ghoranneviss, M. Borghei, *J. Fusion Energ.*, **2011**, 30, 447-452.
5. S. Ghosh, D.K. Avasthi, A. Tripathi, D. Kabiraj, S. Singh, D.S. Misra, *Nucl. Instrum. Methods Phys. Res. B*, **2004**, 219–220, 973–979.
6. Z. Khalaj, S. Z. Taheri, S. N. Laheghi and P. A. Eslami, *IPJ*, **2009**, 3-1, 19.
7. K. Yamazaki, K. Furuichi, I. Tsumura and Y. Takagi, *J. Cryst. Growth*, **2008**, 310, 1019-1022.
8. L.L. Melo, J.R. Moro, R.M. Castro, E.J. Corat and V.J. Trava Airoldi, *J. Surf Coat Tech.*, **2007**, 201, 7382-7386.
9. H. Zhoutong, Y. Shumin, L. Qintao, Z. Dezhang and G. Jinlong, *J. Nucl. Sci. Tech.*, **2008**, 19, 83-87.
10. Yongqing Fu, Bibo Yan, Nee Lam Loh, *Surf. Coat. Technol.*, **2000**, 130, 173-185.
11. H.P. Lorenz, *Diamond Relat. Matter.*, **1995**, 4, 1088-1092.
12. I.Y. Konyashin, M.B. Guseva, V.G. Babaev, V.V. Khvostov, G.M. Lopez, A.E. Alexenko, *Thin Solid Films*, **1997**, 300, 18-24.
13. Z. Khalaj, M. Ghoranneviss, S. Nasirilaheghi, Z. Ghorannevis, R. Hatakeyama, *CJCP*, **2010**, 23, 689-692.